Prediction of blast induced ground vibrations in Karoun III power plant and dam: a neural network

by M. Kamali* and M. Ataei*

Synopsis

In this research, in order to predict the peak particle velocity (PPV) (as vibration indicator) caused by blasting projects in the excavations of the Karoun III power plant and dam, three techniques including statistical, empirical, and neural network were used and their results were interpreted and compared. First, multivariate regression analysis (MVRA) was used as statistical approach. Next, PPV was predicted using some widely used empirical models. Lastly, an artificial neural network was used. In the ANN model, maximum charge per delay, total charge per round, distance from blast site, direction of firing, blasthole length, number of blastholes, total delay in milliseconds, number of delay intervals, and average specific charge were taken into consideration as input parameters and consequently the PPV as output parameter. The results of the techniques were interpreted from two points of view. Firstly, the correlation between the observed data and predicted ones, secondly the total error between observed data and predicted ones. The MVRA had a satisfactory correlation but its error of estimation was comparatively very high. The empirical model had reliable correlation and a small error of estimation; in total the results of empirical method were more reliable than those of MVRA. Generally, the ANN approach showed very high correlation and a very small error. The results of this research indicated that the ANN model is the best predicting model for PPV in comparison with other approaches.

Keywords
Neural network, blasting, peak particle velocity, ground vibration, vibrations monitoring and excavation.

Introduction

One of the by-products of blasting in engineering activities is the blast-produced ground vibrations. If this product of blasting is not controlled, it could potentially damage surrounding structures. Controlling of the blast-produced vibration needs to predict the resulted vibration accurately based on effective parameters such as the characteristics of the blast pattern and site. Thus prediction and control of the vibration are of great importance in engineering activities involving blasting projects.

In theKaroun III power plant and dam, there are several underground excavations which are being developed using drilling and blasting techniques. The resultant vibrations influence the newly constructed concrete structures. For this reason a blast prediction and controlling program seemed to be essential. Therefore a series of field observation and measurements were conducted in the study area.

In order to estimate and analyse the blast vibration effect and consequences, different indicators have been proposed such as: peak particle velocity (PPV), peak particle acceleration (PPA), peak particle displacement (PPD), etc. Of these indictors, the PPV has been used frequently by different authors and standards. For instance, the US Bureau of Mines (USBM) has extensively studied various aspects of ground vibration, etc. caused by opencast blasting and damaging effects on different types of structures. It was found that PPV is the best index to determine the damage criteria for structures[1]. In addition, PPV has been employed as an vibration index in the Indian Standard Institute[2], German DIN Standard 4150[3], Indian CMRI standards[4], Rockwell's Energy Formula[5], Crandell's Energy Ratio Concept[6] and in different empirical PPV predictor models such as: Duval and Petkof[7], Langfors and Kihlstrom[8], Davies *et al.*[9], Ambrases and Hendron[10], Bureau of Indian Standard predictor[11], Ghosh and Daemen[12], Pal Roy[13], Duvall and Fogelson[14], Lundborg[15], Smith and Heteterington[16], Holmberg and Persson[17] and Gupta *et al.*[18].

In this study PPV is also used as the vibration index for estimating the vibration level. In this paper three alternatives are employed to predict PPV. First multivariate regression analysis (MVRA) is used as a statistical approach to predict PPV based on some input parameters and then a few widely-

* *Faculty of Mining, Petroleum and Geophysics Engineering, Shahrood University of Technology, Iran.*

 SA ISSN 0038–223X/3.00 + 0.00. Paper received Aug. 2009; revised paper received Dec. 2010.

used empirical PPV predictors are used; finally a neural network is used to predict the PPV. Eventually the results are interpreted and compared.

Effective parameters on peak particle velocity (PPV)

The intensity of ground vibrations depends on various parameters. These can be broadly divided into two categories, namely, controllable parameters and uncontrollable parameters, as shown in Table I. Controllable parameters can be changed by the blaster in charge, whereas uncontrollable parameters are natural and cannot be controlled[19]. In this study nine parameters that affect the intensity of ground vibration have been taken into account, including maximum charge per delay (*W*), total charge per round (*W*t), distance from blast site (*D*), direction of firing ϕ, blasthole length (*h*), number of blastholes (*N*), total delay in millisecond (*Dt*), number of delay intervals (*ND*), and average specific charge (*S*c). The intensity of vibration is directly proportional to *W*, *W*t, *h*, *N* and it is indirectly proportional to *D*, *Dt*, *ND*.

In most cases, when high blast vibration is encountered, the blasters tend to reduce the specific charge. But after a critical amount of specific charge, the intensity of vibration would increase abruptly[20]. This fact illustrated in Figure 1.

Like specific charge, it cannot be determined whether the intensity of blasting is directly or indirectly proportional to firing direction (angle between recording and blasting points). There is, however, a critical angle in which the recorded blast intensity would peak[20]. Figure 2 illustrates the effect of firing direction. It shows that there is reinforcement in the intensity of the blast-induced vibration at the direction of blasting, whereas at the opposite direction there is no such reinforcement.

Site description and measurement

In order to study of the effects of blast vibrations in Karoun III excavations, data measurement operations were done with seismographs model UVS500 made by Nitro Nobel Company. This device includes 3 parts: the main part, geophone, and connective cables. Device power is supplied by one 1.5 V battery. The device has a hydrometer that will be activated if humidity of measurement area is higher than allowed limits. In this condition, the position of installation must be changed. The geophone can measure particles' velocity in three main directions and resultant amplitude. Also the variation graph of peak particle velocity versus time is accessible.

In order to measure vibration data at one point, in the first stage, the geophone bolt (that ias 25 cm long and 20 mm in diameter) must be installed. For this purpose, after drilling, the bolts would be put in the holes and the experiments could be started after cement grouting has reached the seven-day strength. Because any weakness will decrease the precision of experiments, the place of bolt installation should not have any geological weakness such as alteration, bedding or jointing. After installation of the geophone on the bolt, the device must be connected to the geophone by connective cables and should be put in a safe place. Having carried out the above stages, the device will be ready for measurement. After turning it on, there are 12 minutes for blasting and, after these 12 minutes, the device will be automatically

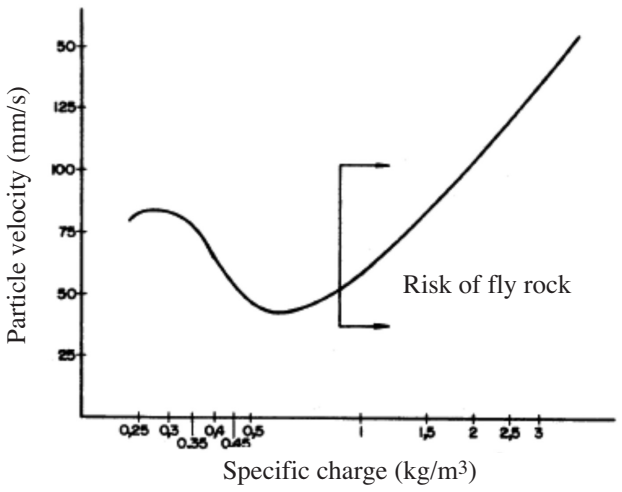

Figure 1. Effect of specific charge on vibration intensity (after Jimeno *et al.* 1995)[20]

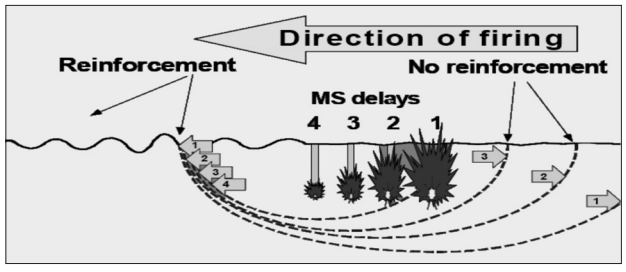

Figure 2—The effect of firing direction

Table I

Controllable and uncontrollable parameters that affect intensity of vibration (after Mohamed, 2009)[19]

Controllable variables				Uncontrollable variables
Geometrical parameters	**Explosive dependent parameters**	**Operational parameters**	**Others**	**Delay time scatter**
Hole diameter Burden Spacing Bench height Stemming Hole inclination Sub-drilling	Explosive type Total explosives Max. charge/delay Explosive energy VOD P-wave in rock	Blast size Initiation point Delay sequence Delay intervals Firing method Confinement	Distance to object	Rock conditions Topography Geology Rock properties Weather conditions

turned off. For this reason, if the blast is not to be executed up to this time, the device must be turned on again. The installation coordinates of the geophone and blast centre must be defined by mapping and surveying precisely in advance. The locations of 11 installed geophones in Karoun III dam and power plant are shown in Figure 3.

For each blasting sequence, maximum charge per delay (W), total charge per round (Wt), distance from blast (D), direction of blasting ϕ, blasthole length (h), number of blastholes (N), total delay in milliseconds (Dt), number of delay intervals (ND), average specific charge (Sc) as input and effective parameters and produced PPV as output have been measured and recorded. In total, 28 records were measured in this region. The statistical summary of input and output parameters is given in Tables II and III, respectively.

Statistical method (multivariate regression analysis)

Multivariate regression analysis (MVRA) was used as a statistical approach to establish a linear relationship between output and input parameters. The MVRA was preformed by using SPSS (15.0) in two models as following:

➤ Model including constant

$$PPV = 0.434\ W + 0.258\ Wt - 0.455\ D + 0.048 - 6.092\ h - 0.547\ N + 26.811\ ND + 0.060\ Sc - 53.98$$

$$R^2 = 0.90 \quad [1]$$

The coefficient of the total delay in milliseconds (Dt) in Equation [1] is zero.

➤ Model without constant

$$PPV = 0.444\ W + 0.268\ Wt - 0.456\ D + 0.048 - 11.149\ h - 0.540\ N + 14.323\ ND + 0.042\ SC$$

$$R^2 = 0.94 \quad [2]$$

The coefficient of total delay in milliseconds (Dt) in Equation [2] is zero.

Empirical PPV predictors

Over years, researchers have conducted different studies to establish the empirical equations in order to predict the PPV[7–18]. The frequently used PPV predictors are listed in Table IV. The empirical and conventional PPV predictor models are basically based on two important variables, maximum charge per delay and distance from blast site. In fact, all these models have been based on scaled distance (SD). The scaled distance is the hybrid variable of D and W (in all formulas W and D refer to maximum charge per delay and distance from blast site). The general equation of scaled distance is as follows:

Table II

Statistical summery of input parameters

Input parameter	Unit	Min.	Max.	Mean	S.dev.
Max. charge per delay (W)	kg	22.5	72.25	42.39	13.06
Total charge per round (Wt)	kg	140.5	420	266.65	56.25
Distance from blast (D)	m	32.18	173.9	95.63	46.60
Direction of blasting (ϕ)	Degree	0	159	65.36	47.77
Blast hole length (h)	m	3	6	3.56	0.62
No. of blast holes (N)	-	15	248	116.8	43.01
Total delay in millisecond (Dt)	ms	875	1375	1266.66	173.00
No. of delay intervals (ND)	-	7	11	10.13	1.38
Average specific charge (Sc)	(kg/ m^3)	0.65	1.98	1.32	0.32

Table III

Statistical summary of output parameter

Output parameter	Unit	Min.	Max.	Mean	S.dev.
Peak particle velocity (PPV)	mm/s	0.3	71	21.16	28.13

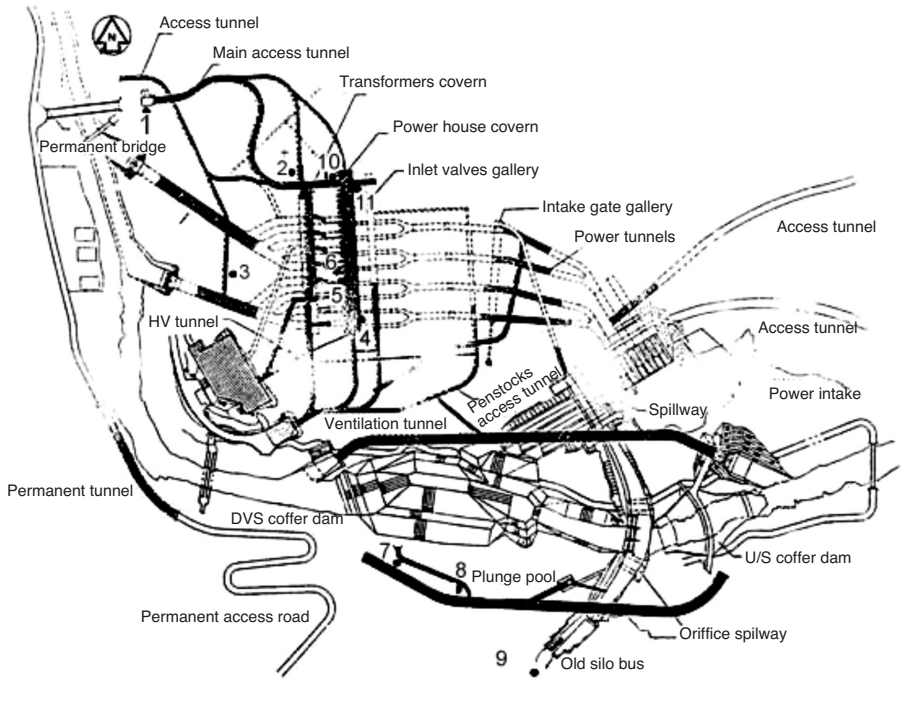

Figure 3—Situation of 11 geophones installed in Karoun III power plant and dam

Table IV

Frequently used conventional PPV predictors

Predictor	Year	Equation	Ref.
USBM	1959	$PPV = K\left(\frac{D}{\sqrt{W}}\right)^{-B}$	[7]
Langfors–Kihlstrom	1963	$PPV = K\left(\sqrt{\frac{W}{\sqrt{D^{2/3}}}}\right)^{B}$	[8]
General predictor	1964	$PPV = K.D^{-B}.W^{A}$	[9]
Ambrases-Hendron	1968	$PPV = K\left(\frac{D}{\sqrt[3]{W}}\right)^{-B}$	[10]
Bureau of Indian Standard	1973	$PPV = K\left(\frac{W}{D^{2/3}}\right)^{B}$	[11]
Ghosh–Daemen	1983	$PPV = K\left(\frac{D}{\sqrt{W}}\right)^{-B}.e^{-\alpha D}$	[12]
CMRI	1993	$PPV = n + K\left(\frac{D}{\sqrt{W}}\right)^{-1}$	[13]

$$SD = \frac{W^{k_1}}{D^{k_2}} \quad [3]$$

where k_1 and k_2 are predefined for each particular predictor.

For parameter estimation in these predictors, simple regression analysis was used, except for the general predictor and Ghosh–Daemen models. In order to establish linear equations, their equations were changed as following:

- General predictor

$$PPV = K.D^{-B}.W^{A} \quad [4]$$

$$\ln(PPV) = \ln\left(K.D^{-B}.W^{A}\right) \quad [5]$$

$$\ln(PPV) = \ln(K) - B\ln(D) + A\ln(W) \quad [6]$$

- Ghosh – Daemen predictor

$$PPV = K\left(\frac{D}{\sqrt{W}}\right)^{-B}.e^{-\alpha D} \quad [7]$$

$$\ln(PPV) = \ln(K\left(\frac{D}{\sqrt{W}}\right)^{-B}.e^{-\alpha D}) \quad [8]$$

$$\ln(PPV) = \ln(K) - B\ln\left(\frac{D}{\sqrt{W}}\right) - \alpha D \quad [9]$$

Then, by using multinomial linear regression analysis, the constant parameters were estimated using SPSS (15.0) software.

The parameter estimation and goodness-of-fit results for the predictors are given in Table V. Figures 4(a), (b), (c), (d) and (e) show the obtained curves of two-dimensional PPV predictor models.

Two important indexes showing the accuracy and reliability of each model have been listed in Table V, the indexes are the correlation index (i.e. R^2) and the index of error estimation, i.e. MSE (mean squared error). The MSE error function is calculated as below:

$$MSE = \sum_{i=1}^{n}\frac{e_i^2}{n} \quad [10]$$

where e is the error between ith observed data and predicted one. n is the number of observed data.

To compare the indexes of the predictors, Figures 5 and 6 illustrate the correlation and MSE error for each model graphically; these indexes determine the reliability and prediction precision of any predictors. For instance, the general predictor has the highest correlation or R^2 but the CMRI predictor has the least MSE error or the error of estimation. Although the correlation of the general predictor is 0.01 more than that of the CMRI predictor, the MSE error of CMRI predictor is 47.84 less than that of the general predictor. Thus, both of these indexes should be simultaneously (not separately) used to select the best predictor.

Artificial neural network (ANN)

An artificial neural network (ANN) is a collection of nodes and links among these nodes. It is massive parallel network of nodes. The weights given to different links play a major role in processing inputs and outputs. The way of interconnection among the processing elements determines the network architecture[21].

Table V

Parameter estimation and goodness-of-fit for the predictors

Predictor	K	B	A		n	Correlation (R^2)	MSE (mean squared error)
USBM	3621.8	2.6551	-		-	0.90	60.89
Langfors–Kihlstrom	0.3192	6.7393	-		-	0.88	206.30
General predictor	91.83	2.57	2.22		-	0.92	108.28
Ambrases-Hendron	18484	2.6529	-		-	0.88	72.89
Bureau of Indian Standard	0.3192	3.3697	-		-	0.88	196.35
Ghosh–Daemen	2.22	3.55	-	0.012	-	0.91	1147.69
CMRI	373.39	-	-	-	-17.921	0.91	60.44

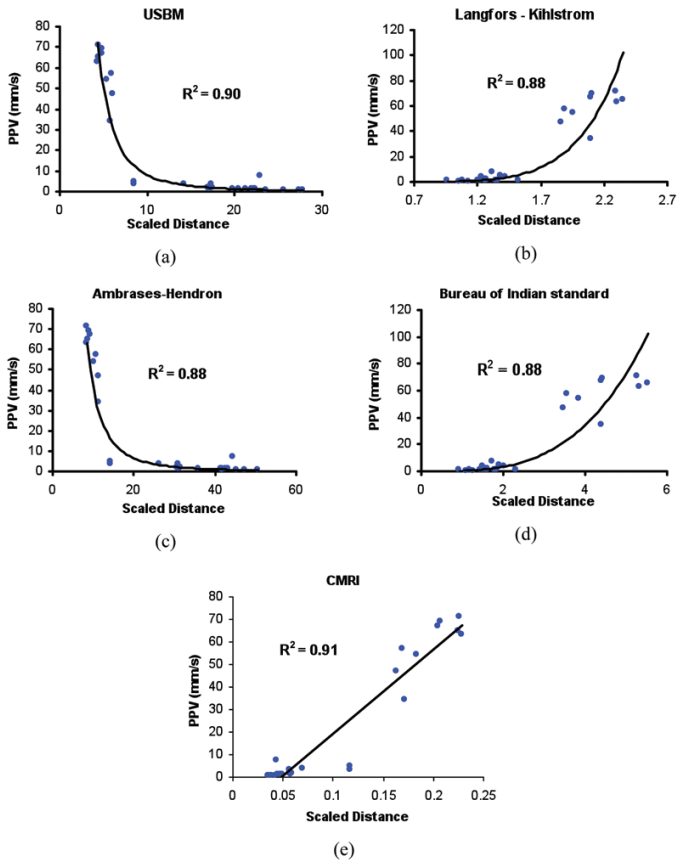

Figure 4—The curves of 2-dimentional empirical models (a) USBM, (b) Langfors – Kihlstrom, (c) Ambrases-Hendron, (d) Bureau of Indian standard, (e) CMRI

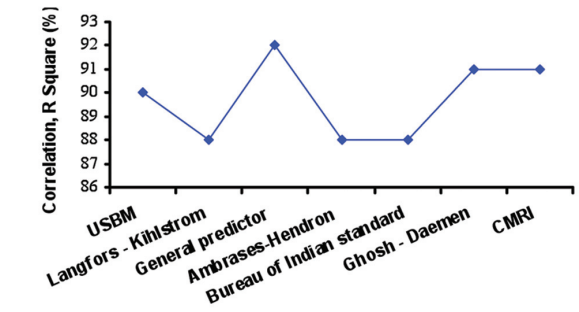

Figure 5—Correlation between empirical models and observed data

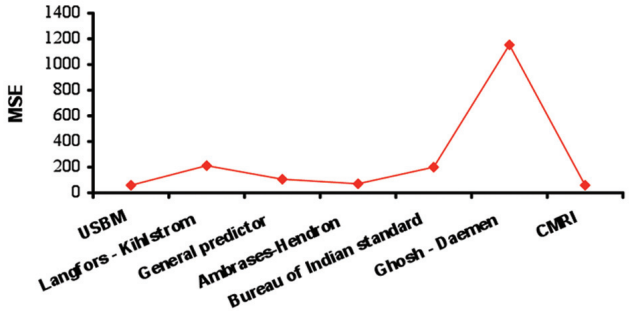

Figure 6—MSE error of empirical models

Over years neural models have been used in different fields to solve the complicated problems when conventional alternatives weren't capable of solving. The application of ANN models in different fields of mining and civil engineering and especially in the blast-produced vibration prediction have been listed in Tables VI and VII, respectively.

All these applications emphasize the fact that ANN models are such powerful and adaptive approaches to model the different problems when the conventional approaches are unable. In this study a neural network is also employed as an alternative to predict the PPV based on nine input parameters.

Network architecture

To select the proper architecture, it is almost impossible to find the best-fit network types by trying all network type. This is because each network type has particular properties that can be used to solve a particular problem, but there is no general rule to determine which is the best-fit network. It is also time consuming to try all. The alternative is to use experience or a role of thumb.

In this study a feed-forward back-propagation neural network was used. The characteristics of the ANN architecture are as follows:

- Network type = Feed-forward back-propagation
- Training function = Levenberg-Marquardt back-propagation

Table VI

ANN applications in different fields of mining and civil engineering

Author(s)	Year	Application	Ref.
Dysart and Pulli	1990	ANN used to classify the regional seismic event at the noress array	[22]
Yang and Zhang	1997	Investigation of the point load testing using ANN model	[23]
Cai and zZhao	1997	Using ANN for tunnel design, optimal selection of rock support and stability assessment of tunnel	[24]
Rudajev *et al*.	1996 and 1999	Determining event types such as earthquake, mining blasts, chemical explosions, etc., from seismological data using ANN	[25–27]
Maulenkamp and Grima	1999	Development of a model by which uniaxial compressive strength could be predicted using ANN	[28]
Singh *et al*.	2001	Prediction of the strength of schistose rocks using ANN	[29]
Khandelwal and Singh	2002	Investigation of stability of waste dump slopes by using ANN	[30]
Ambrozic *et al*.	2003	Using ANN approach to predict the subsidence due to underground mining	[31]
Deng *et al*.	2003	Combination of the three approaches, namely finite element methods, neural networks, and reliability to design pillar	[32]
Maity and Saha	2004	Assessment of the damage in structures because of variation of static parameters	[33]
Singh *et al*.	2004	Investigation of P-wave velocity and anisotropic property of rocks with ANN	[34]
Monjezi *et al*.	2006	Prediction by ANN of the ratio of muck pile before and after the blast, fly rock, and total explosive used in the blasting operation	[35]
Monjezi and Dehghani	2008	Evaluation of the effect of blasting pattern parameters on back break using neural networks	[36]
Qiang Wu *et al*.	2008	Prediction of the size-limited structures in a coal mine using artificial neural networks	[37]

Table VII

ANN applications in blast-produced vibration prediction

author(s)	Year	Application	Ref.
Chakraborty *et al*.	2004	Studied the effectiveness of multilayer perceptron neural networks for prediction of the blasting vibration along with different empirical models	[38]
Singh	2004	Employed a feed-forward back-propagation neural network approach for prediction and control of ground vibrations in mines	[39]
Singh and Virendra Singh	2005	Employed an intelligent approach to prediction and control ground vibration in mines and also used MVRA as statistical approach, then compared the results.	[21]
Khandelwal and Singh	2006	Prediction of blast-induced ground vibrations and frequency in opencast mine using an ANN model	[40]
Khandelwal and Singh	2007	Evaluation of blast-induced ground vibration predictors using ANN models	[41]
Khandelwal and Singh	2009	Using the neural network to predict the blast-induced vibrations	[42]

- Number of layers = 3
- Number of neurons in hidden layer = 15
- Number of neurons in input layer = 9
- Number of neurons in output layer = 1.

The ANN architecture used is illustrated in Figure 7.

To perform the ANN model MATLAB software was used. The analysis was performed during two stages, namely: training and validation.

- *Training stage*—the observed data-set including 28 samples was divided into two sets: The training data-set and validation data-set. The training data-set contains 20 samples and validation data-set contains the remaining 8 samples. In the training stage the network is trained only by using training data-set. Figure 8 shows the training process during epochs. The training process is stopped as soon as one of the stopping criteria is satisfied. The observed data and data predicted by the trained ANN model are compared in Table VIII. Figure 9 shows the correlation between observed data and data predicted by the trained ANN model.

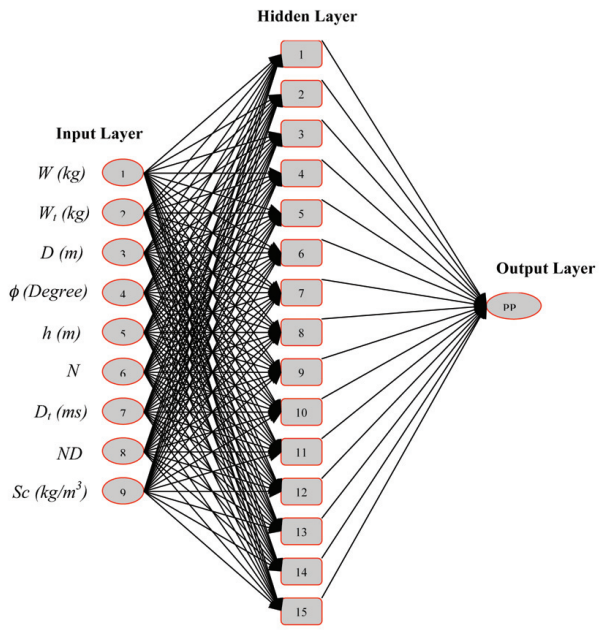

Figure 7—ANN architecture

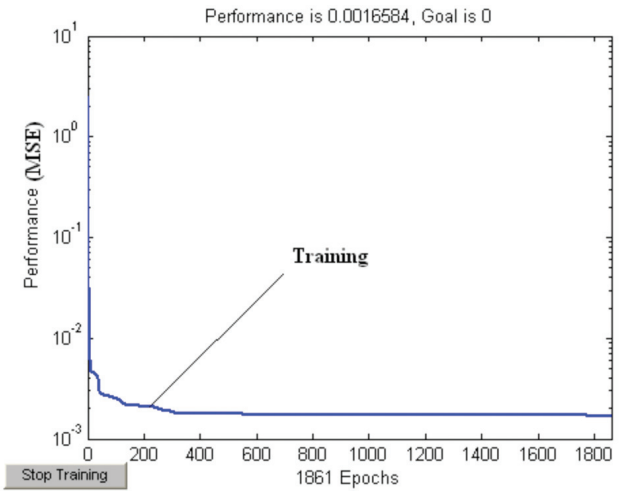

Figure 8—Trained network

Table VIII

Observed data and predicted by the trained ANN model

Observed data	Predicted by ANN model	Error
0.7	0.67	0.03
1.1	1.38	0.28
0.3	0.33	0.03
3.3	3.30	0
0.6	0.69	0.09
0.4	0.85	0.45
1	1	0
4.7	4.89	0.19
3.7	5	1.3
3.3	3.31	0.01
1.2	1.56	0.36
34	34.74	0.74
54	55.43	1.43
65	65.01	0.01
1.3	1.15	0.15
1.5	2.1	0.6
71	71.03	0.03
63	68.25	5.25
69	70.00	1
67	67.9	0.9

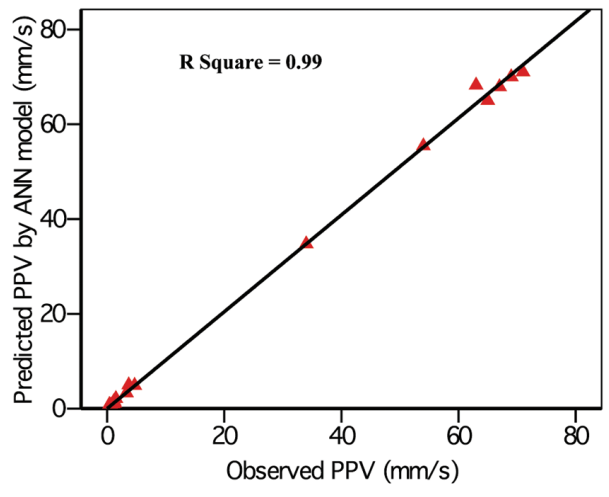

Figure 9—Correlation between the observed data & predicted in training stage

- *Validation stage*—during the training stage the network might learn too much. This problem is referred to as over-fitting. Over-fitting is a critical problem in almost all standard NNs architecture[43]. One of the solutions is early stopping[44], but this approach needs more critical attention as this problem is harder than expected[43].

Hence, for this problem during training, the validation data-set is associated with the training data-set. After a few epochs the network is tested with the validation data. The training is stopped as soon as the error in the validation data-set increases rapidly higher than the last time it was checked[45]. Figure 10 shows that the training should stop at a point when the validation error starts to increase.

Figure 11 shows the training and validation processes during epochs. Unlike the training stage, here the training process is stopped as soon as the error in the validation data-set increases rapidly higher than the last time it was checked. The observed data and data predicted by the trained ANN model are compared in Table IX for validation and training data-sets. Figures 12 and 13 show the correlation between observed data and data predicted by the trained ANN model for validation and training data-sets.

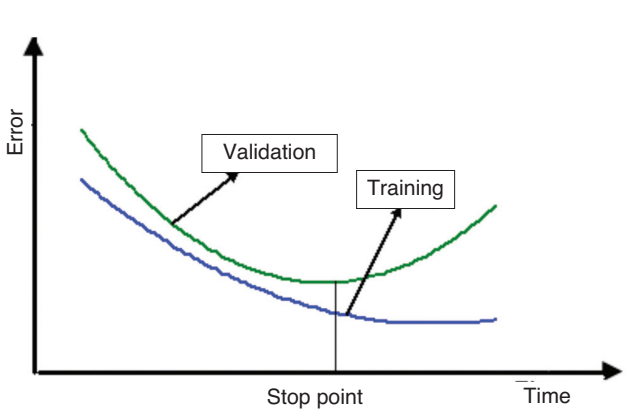

Figure 10—Training and validation curve

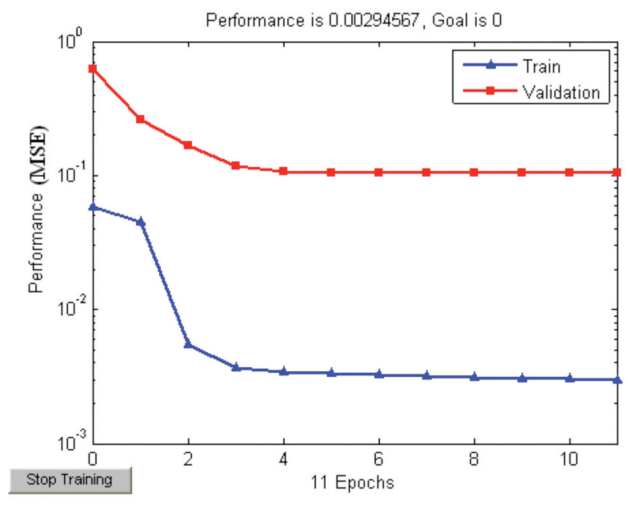

Figure 11—Trained and validated network

Table IX

Observed data and data predicted by ANN model for training and validation data-sets

Training data-set			Validation data-set		
Observed data	**Predicted by ANN model**	**Error**	**Observed data**	**Predicted by ANN model**	**Error**
0.7	0.85	0.15	57	45.60	11.4
1.1	1.86	0.76	47	47.52	0.52
0.3	0.80	0.5	1.3	2.14	0.84
3.3	3.30	0	1.7	1.75	0.05
0.6	1.2	0.6	0.9	0.63	0.27
0.4	0.89	0.49	1.2	2.45	1.25
1	1.06	0.06	1.1	1.17	0.07
4.7	4.65	0.05	7.2	7.68	0.48
3.7	6.3	2.6			
3.3	3.32	0.02			
1.2	1.34	0.14			
34	36.98	2.98			
54	49.85	4.15			
65	64.36	0.64			
1.3	1.21	0.09			
1.5	1.48	0.02			
71	75.55	4.55			
63	56.45	6.55			
69	68.41	0.59			
67	72.1	5.1			

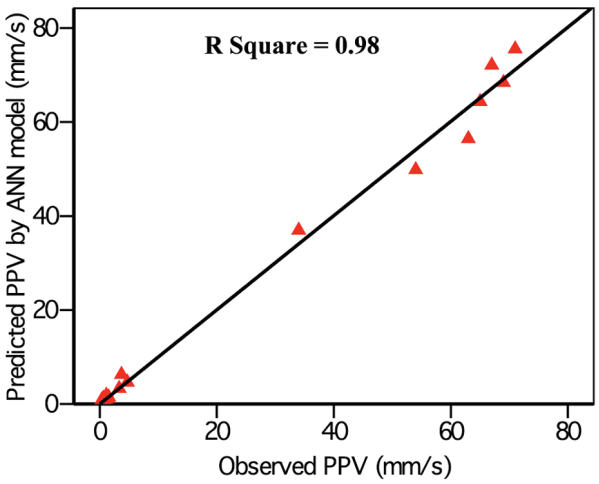

Figure 12—Correlation between the observed data and data predicted in validation stage (for training data-set)

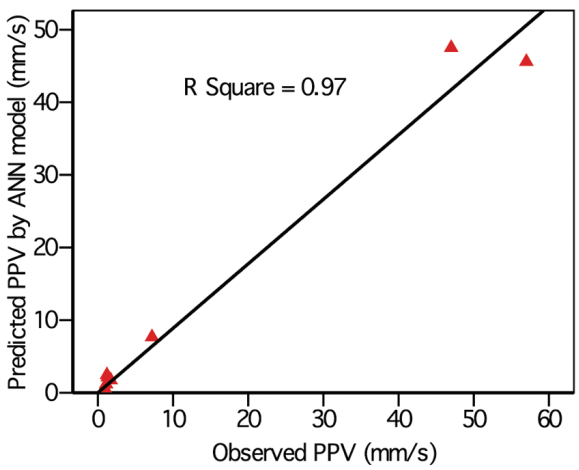

Figure 13—Correlation between the observed data and data predicted in validation stage (for validation data-set)

Results and discussion

By considering the results of the approaches used to predict the PPV, it can be seen that ANN technique has the highest $R^2 = 0.98$ for the given problem, after that MVRA with $R^2 = 0.94$, and finally the general predictor of empirical predictors with $R^2 = 0.92$. But a high R^2 indicates only that correlation between the observed and predicted data are high, it does not mean that the observed data are close to the predicted data. In other words R^2 is not a suitable index or able to show errors between them. By considering just R^2, the ranking of these methods would be: ANN, MVRA, and general predictor.

As stated before, another index is required to indicate the estimation error of each predictor. Here the MSE error is used, given in Equation [10]. In empirical models, Figures 5 and 6 illustrate the correlation (R^2) and MSE error for each model; these indexes determine the reliability and prediction precision of any predictors. In these figures, general predictor has the highest correlation or R^2 but the CMRI predictor has the least MSE error or the error of estimation. Although the correlation of the general predictor is 0.01 more than that of the CMRI predictor, the MSE error of the CMRI predictor is 47.84 less than that of the general predictor. Based on engineering judgement, the CMRI predictor is selected as the best empirical predictor.

Figure14 compares the obtained results of the best-fit empirical equation, MVRA and ANN with observed data. This figure shows that although MVRA has greater R^2, it shows a wide range of estimation errors. From this figure it can be easily seen that ANN has the most correlation and the least error, thus it is chosen as the most reliable model.

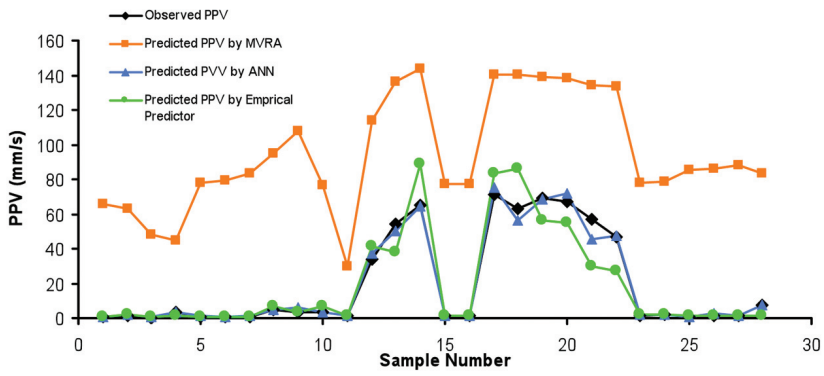

Figure 14—Comparison error between observed data and predicted by three models

Table X

Correlation and MSE error of the used models

Prediction model	Correlation (R2)	MSE (Mean squared error)
AAN model	0.98	9.19
MVRA	0.94	5443.67
Best empirical model (CMRI)	0.92	60.44

Again, this study indicates that the ANN model has great adaptability. Table X gives the exact values of the MSE error and R^2. By considering Table X and using engineering judgement, the best empirical model (CMRI) is superior to the MVRA approach. Although the ANN model is the best-fit model, the results of the empirical models are reliable and satisfactory and can be considered as a solution.

Conclusion

In this paper three techniques, i.e. ANN, MVRA, and empirical, have been used to predict the blast-induced PPV in the structures of the Karoun III power plant and dam. After analysis, it was found that the ANN model is the best predictor model using a novel methodology. The most important point which has been taken into consideration in this methodology is that the R square (R^2) is not a reliable and suitable index to show and validate the precision of the prediction of a proposed model. The high R^2 shows only that the outputs of the proposed model are highly correlated to the measured and observed data. It does not mean that these two groups of data are close to each other or that; the error between them is small. To select the proper model in any case, these two indexes (R^2 and an error function such as MSE) should be simultaneously taken into account, and based on engineering judgement, the proper model would be chosen. In this paper the ANN model has the highest R^2 and the least MSE error. Thus it was selected as the best model. But between empirical models and the MVRA model, the empirical model (CMRI predictor) was selected as the second model using engineering judgement. This methodology is first employed in this paper to interpret the results of a model.

Acknowledgment

The authors express their gratitude for support given to the study by the University of Technology of Shahrood. Special thanks to M.Rahideh, A.Modares, F.Jafari, A.Talebi for assisting.

References

1. Basu, D. and Sen, M. Blast induced ground vibration norms—A critical review, *National Seminar on Policies, Statutes & Legislation in Mines*, 2005.

2. Indian Standard Institute. Criteria for safety and design of structures subjected to underground blast, *ISI Bull* 1973, IS-6922.

3. New BM. Ground vibration caused by civil engineering works. Transport and Road Research Laboratory, *Research Report 53*, 1986, p. 19

4. CMRI .Vibration standards, Central Mining Research Institute, Dhanbad; 1993.

5. Kahriman, A. Analysis of Ground Vibrations Caused by Bench Blasting at Can Open-pit Lignite Mine in Turkey. *Environmental Geology*, vol. 41, 2001. pp. 653–661.

6. Crandell, F.J. Ground vibration due to blasting and its effect upon structures. *Journal of Boston society of civil engineers*, 1949.

7. Duvall, W.I. and Petkof, B. Spherical propagation of explosion generated strain pulses in rock. *USBM Report of Investigation* 5483, 1959, p. 21.

8. Langefors, U. and Kihlstrom, B. *The modern technique of rock blasting*. New York, Wiley, 1963.

9. Davies, B., Farmer, I.W., and Attewell, P.B. Ground vibrations from shallow sub-surface blasts. *The Engineer*, London 1964, pp. 553–9.

10. Ambraseys, N.R. and Hendron, A.J. *Dynamic behaviour of rock masses: rock mechanics in engineering practices*. London: Wiley, 1968.

11. Bureau of Indian Standard. Criteria for safety and design of structures subjected to underground blast. ISI Bull IS-6922, 1973.

12. Ghosh, A. and Daemen, J.K. A simple new blast vibration predictor. *Proceedings of the 24th US symposium on rock mechanics*, College Station, Texas, 1983. pp. 151–161.

13. Pal Roy, P. Putting ground vibration predictors into practice. *Colliery Guardian,* vol. 241, 1993. pp. 63–7.

14. Duvall, W.I. and Fogelson, D.E. Review of criteria for estimating damage to residences from blasting vibration. US Bureau of Mines R.I. 5968, 1962.

15. Lundborg, N. Keeping the lid on flyrock in open-pit blasting. *E/MJ*, May, 1957.

16. Smith, P.D. and Hetherington, J.G. *Blast and ballistic loading of stracture*. Elsevier Science. Butterworth-Heinemann Ltd., Oxford, 1994.

17. Holmberg, R. and Persson, P.A. Design of tunnel perimeter blasthole patterns to prevent rock damage. *Proc. IMM Tunnelling '79 Conference*, London, 1979, pp. 280–283.

18. Gupta, R.N., Pal Roy., P., and Singh, B. Prediction peak particle velocity and air pressure generated by buried explosion. *Int. J. of mining and geological engineering*. 1988.

19. Mohamed, M.T. Artificial neural network for prediction and control of blasting vibrations in Assiut (Egypt) limestone quarry. *International Journal of Rock Mechanics & Mining Sciences,* vol. 46, 2009. pp. 426–431.

20. Jimeno, L.C., Jimeno, L.E., and Carcedo, A.J.F. *Drilling and Blasting of Rocks*, A.A. Balkema, Rotterdam, 1995, pp. 333–365.

21. Singh, T.N. and Singh, V. An intelligent approach to prediction and control ground vibration in mines. *Geotechnical and Geological Engineering,* vol. 23, 2005 pp. 249–262. doi 10.1007/s10706-004-7068-x.

22. Dysart, P.S. and Pulli, J.J. Regional seismic event classification at the noress array: seismological measurements and the use of trained neural networks. *Bull Seismol Soc Am,* vol. 80, 1990. pp. 1910–33.

23. Yang, Y. and Zhang, Q. Analysis for the results of point load testing with artificial neural network. *Proceedings of computing methods and advances in geomechanics*, IACMAG, China, 1997, pp. 607–12.

24. Cai, J.G. and Zhao, J. Use of neural networks in rock tunneling. *Proceedings of computing methods and advances in geomechanics*, IACMAG, China, 1997, pp. 613–618.

25. Rudajev, V. and Ciz, R. Estimation of mining tremor occurrence by using neural networks. *Pure Appl Geophys*, vol. 154, 1999. pp. 57–72.

26. Finnie, G.J. Using neural networks to discriminate between genuine and spurious seismic events in mines. *Pure Appl Geophys*, vol. 154, 1999. pp. 41–56.

27. Musil, M. and Plesinger, A. Discrimination between local micro earthquakes and quarry blasts by multi-layer perceptrons and Kohonen maps. *Bull Seismol Soc Am,* vol. 86, 1996. pp. 1077–90.

28. Maulenkamp, F. and Grima, M.A. Application of neural networks for the prediction of the unconfined compressive strength (UCS) from Equotip Hardness. *Int J Rock Mech Min Sci, vol.* 36, 1999. pp. 29–39.

29. Singh, V.K., Singh, D., and Singh, T.N. Prediction of strength properties of some schistose rock. *Int J Rock Mech Min Sci,* vol. 38, 2001. pp. 269–84.

30. Khandelwal, M. and Singh, T.N. Prediction of waste dump stability by an intelligent approach. *Proceedings of the national symposium on new equipment–new technology, management and safety*, ENTMS, Bhubaneshwar, 2002, pp. 38–45.

31. Amborzic, T. and Turk, G. Prediction of subsidence due to underground mining by artificial neural networks. *Computers & Geosciences*, vol. 29, 2003. pp. 627–637.

32. Deng, J., Yue, Z.Q., Tham, L.G., and Zhu, H.H. Pillar design by combining finite element methods, neural networks and reliability: a case study of the Feng Huangshan copper mine, China. *International Journal of Rock Mechanics & Mining Sciences,* vol. 40, 2003. pp. 585–599.

33. Maity, D. and Saha, A. Damage assessment in structure from changes in static parameters using neural networks. *Sadhana,* vol. 29, 2004. pp. 315–27.

34. Singh, T.N., Kanchan, R., Saigal, K., and Verma, A.K. Prediction of P-wave velocity and anisotropic properties of rock using Artificial Neural Networks technique. *J Sci Ind Res,* vol. 63, 2004. pp. 32–8.

35. Monjezi, M., Singh, T.N., Khandelwal, M., Sinha,S., Singh, V., and Hosseini, I. Prediction and analysis of blast parameters using artificial neural network. *Noise Vib Worldwide*, vol. 37, 2006. pp. 8–16.

36. Monjezi, M. and Dehghani, H. Evaluation of effect of blasting pattern parameters on back break using neural networks. *International Journal of Rock Mechanics & Mining Sciences,* vol. 45, 2008. pp. 1446–1453.

37. Qiang, W., Siyuan, Y., and Jia, Y. The prediction of size-limited structures in a coal mine using Artificial Neural Networks. *International Journal of Rock Mechanics & Mining Sciences* vol. 45, 2008. pp. 999–1006.

38. Chakraborty, A.K., Guha, P., Chattopadhyay, B., Pal, S., and Das, J. *A Fusion Neural Network for Estimation of Blasting Vibration*. N.R. Pal *et al*. (eds.): ICONIP 2004, LNCS 3316, pp. 008.1013, 2004. Springer-Verlag Berlin Heidelberg 2004.

39. Singh, T.N. Artificial neural network approach for prediction and control of ground vibrations in mines. *Mining Technology* (Trans. Inst. Min. Metall. A) September 2004, vol. 113. pp. 251–255. DOI 10.1179/037178404225006137.

40. Khandelwal, M. and Singh, T.N. Prediction of blast induced ground vibrations and frequency in opencast mine: A neural network approach. *Journal of Sound and Vibration,* vol. 289, 2006. pp. 711–725.

41. Khandelwal, M. and Singh, T.N. Evaluation of blast-induced ground vibration predictors. *Soil Dynamics and Earthquake Engineering,* vol. 27, 2007. pp. 116–125. doi:10.1016/j.soildyn.2006.06.004

42. Khandelwal, M. and Singh, T.N. Prediction of blast-induced ground vibration using artificial neural network. *Int J Rock Mech Mining Sci,* 2009. doi:10.1016/j.ijrmms.2009.03.004.

43. Lawrence, S., Giles, C.L., and Tsoi, A.C. Lessons in Neural Network Training: Training May be harder than Expected. *Proceedings of the Fourteenth National Conference on Artificial Intelligence,* AAAI-97, Menlo Park, California: AAAI Press, 1997, pp. 540–545.

44. Sarle, W. Stopped Training and Other Remedies for Overfitting. *Proceedings of the 27th Symposium on the Interface of Computing Science and Statistics*, 1995, pp. 352–360.

45. Prechelt, L. Early Stopping-but when? Neural Networks: Tricks of the trade, Springer Berlin/Heidelberg, vol. 1524, 1998. pp. 55–69. ◆